Modelling and understanding multiple roles of sediment transport in floods

Mingfu Guan
PhD candidate, University of Leeds, Leeds, LS2 9JT, UK. Email: cnmg@leeds.ac.uk

Nigel G. Wright
Professor, University of Leeds, Leeds, LS2 9JT, UK. Email: N.G.Wright@leeds.ac.uk

P. Andrew Sleigh
Senior Lecturer, University of Leeds, Leeds, LS2 9JT, UK. Email: P.A.Sleigh@leeds.ac.uk

ABSTRACT: Outburst floods are characterised by being sudden, short-lived and containing high energy. Such kinds of outburst floods generally comprise an intense advancing water wave which can induce considerable sediment loads. Therefore, it is necessary to incorporate sediment transport effects in flood models, instead of just considering water flow. In this paper, a layer-based morphodynamic model is presented. Of course, a model can never represent all the features in the real world exactly; the model here is mainly developed for sheet flow. The model system is composed of a combination of several modules: 1) a hydrodynamic module governed by 2D Shallow Water equations involving sediment effects; 2) a sediment transport module controlling the mass conservation of sediment; 3) a bed deformation module for updating the bed elevation due to erosion and deposition. For applications, a small-scale dyke breach due to flow overtopping and a large-scale volcano-induced glacial lake outburst flood (GLOF) are simulated by the computational model. Modelling results indicate that sediment transport plays multiple roles in the hydraulic events. In some cases, it delays the onset of flow, changing the flow hydrograph. Nonetheless, in other cases, the flood propagation is accelerated due to the incorporation of sediment transport; conversely, the powerful outburst floods induce sediment into motion and cause rapid geomorphic change of river bed, e.g. millions of cubic meters of sediment are eroded and re-deposited for the volcano-induced GLOF event.

KEY WORDS: layer-based model, sediment transport, fluvial process, flash floods, GLOF.

1 INTRODUCTION

Flash floods are one of the most catastrophic natural hazards for people and infrastructure, including intense rainfall induced floods, dam break floods, glacial outburst floods and sudden release of meltwater from ice sheets caused by volcanic activity etc. (Alho et al. 2005; Carrivick et al. 2010; Carrivick and Rushmer 2006; Manville et al. 1999). Such high-magnitude sudden onset floods generally comprise an advancing intense kinematic water wave which can induce considerable sediment loads, thereby causing rapid geomorphic change. Therefore, the exploration and investigation of such floods cannot be limited to water flow alone, but flow-induced sediment transport should also be incorporated. In recent decades, attention has increasingly been paid to numerical modelling of such floods because it is money-saving and convenient to implement. Although the quantification of geomorphic change is unattainable completely, at least they enhance and improve the insights of people into the effects of sediment transport in rapid geomorphic floods. To date, a variety of morphodynamic models have been developed to emphasize the erosion and deposition by outburst floods (Capart and Young 1998; Fraccarollo and Capart 2002; Wu and Wang 2007; Xia et al. 2010). Most of them are mainly focused on small-scale experimental events; and it is found that sediment plays a role in reducing flow velocity and increasing the maximum water depth. However, the resulting understanding of sediment effects is not universally applicable. In reality, sediment may play multiple roles in either delaying the flood propagation or accelerating the flooding process. Based

on those considerations, this paper presents a computational model for rapid geomorphic floods, analyses and evaluates the multiple implications of sediment transport on the flooding process from numerical results of a small-scale case and a large-scale flood.

2 HYDRO-MORPHODYNAMIC MODEL

A layer-based sheet flow model has been presented and validated by the authors (Guan et al. 2013a). This model is used in the paper. The framework for the layer-based model system is considered as constituting of:

- a layer-based conceptual model
- a hydrodynamic model governed by the 2D shallow water equations with sediment effects;
- a sediment transport model controlling the sediment mass conservation, and
- a bed deformation model for updating the bed elevation under the erosion and deposition

Sediment transport in practical engineering problems is a rather complex process. Of course, a model can never represent all the features in the real world exactly; without exception, the model system also made some assumptions. (1) Non-cohesive sediment material is considered. (2) The collision effects between particles and particles are ignored. (3) The time scale of bed change is much larger than that of flow movement so that the flow is calculated assuming a "fixed" bed at each time step.

2.1 Hydrodynamic Model

The hydrodynamic process is governed by the 2D Shallow Water equations, involving the mass and momentum exchange between flow and sediment, which are written as:

$$\frac{\partial \eta}{\partial t}+\frac{\partial hu}{\partial x}+\frac{\partial hv}{\partial y}=0 \tag{1}$$

$$\frac{\partial hu}{\partial t}+\frac{\partial}{\partial x}\left(hu^2+\frac{1}{2}gh^2\right)+\frac{\partial huv}{\partial y}=gh\left(S_{ox}-S_{fx}\right)+\frac{\Delta\rho u}{\rho}\frac{\partial z_b}{\partial t}\left(\frac{1-p}{\beta}-C\right)-\frac{\Delta\rho gh^2}{2\rho}\frac{\partial C}{\partial x}-S_A \tag{2a}$$

$$\frac{\partial hv}{\partial t}+\frac{\partial huv}{\partial x}+\frac{\partial}{\partial y}\left(hv^2+\frac{1}{2}gh^2\right)=gh\left(S_{oy}-S_{fy}\right)+\frac{\Delta\rho u}{\rho}\frac{\partial z_b}{\partial t}\left(\frac{1-p}{\beta}-C\right)-\frac{\Delta\rho gh^2}{2\rho}\frac{\partial C}{\partial y}-S_B \tag{2b}$$

where h= flow depth; z_b= bed elevation; η=water surface; u, v= average flow velocity in x and y direction; p= sediment porosity; C= volumetric concentration in flow depth; ρ_s, ρ_w= density of sediment and water respectively; $\Delta\rho=\rho_s-\rho_w$; ρ= density of sediment-flow mixture; β= u/u_s= flow-to-sediment velocity ratio determined by the equation proposed by(Greimann et al. 2008); S_A, S_B are the additional terms related to the velocity ratio β.

$$S_{A,B}=\frac{\Delta\rho \mathrm{U}}{\rho}\left[\left(1-\frac{1}{\beta}\right)\left(C\frac{\partial hu}{\partial x}+C\frac{\partial hv}{\partial y}\right)-\left(1-\frac{1}{\beta}\right)\left(hu\frac{\partial C}{\partial x}+hv\frac{\partial C}{\partial y}\right)\right] \tag{3}$$

where U=u for S_A; U=v for S_B; S_{ox}, S_{oy} = bed slopes; S_{fx}, S_{fy} = frictional slopes calculated by $S_{fx}=n^2u\sqrt{u^2+v^2}/h^{4/3}$; $S_{fy}=n^2v\sqrt{u^2+v^2}/h^{4/3}$.

2.2 Sediment Transport Model

For non-uniform sediment transport, the mass equation of the ith sediment class in sheet flow layer is written by

$$\frac{\partial hC_i}{\partial t}+\frac{1}{\beta}\frac{\partial huC_i}{\partial x}+\frac{1}{\beta}\frac{\partial hvC_i}{\partial y}=-\frac{1}{\beta}\frac{(q_{bi}-F_iq_{b*i})}{L_i} \tag{4}$$

where F_i = the proportion of the ith size class; q_{bi}, q_{b*i}, C_i and L_i = sediment transport rate, total transport capacity, volumetric concentration, and non-equilibrium adaptation length of the ith size class respectively; and $C=\sum_{i=1}^{N}C_i$. For the non-uniform sediment, we calculate the sediment transport capacity according to the classification of size fractions, and then sum the proportion of each size class as:

$$q_{b*}=\sum_{i=1}^{N}F_iq_{b*i} \tag{5}$$

where q_{b*} = sediment transport capacity in total. The modified Meyer-Peter & Müller equation (Meyer-Peter and Müller 1948) with a calibrated coefficient ψ is used for the gentle bed slope smaller than 0.03, and the equation by (Smart and Jäggi 1983) is applied for the steep slope greater than 0.03with a limitation of maximum S_o to be 0.20.

$$q_{b*i} = \psi 8\left(\theta_i - \theta_{c,i}\right)^{1.5}\sqrt{(s-1)gd_{50}^3} \quad 0 \le S_o < 0.03 \tag{6}$$

$$q_{b*i} = 4\left(\frac{d_{90}}{d_{30}}\right)^{0.2}\frac{h^{1/6}}{n\sqrt{g}}min(S_o, 0.2)^{0.6}\theta_i^{0.5}\left(\theta_i - \theta_{c,i}\right)\sqrt{(s-1)gd_{50}^3}\,S_o \ge 0.03 \tag{7}$$

in which, θ_{ci}= critical dimensionless bed shear stress of ith fraction; θ_i= dimensionless Shields parameter of ith fraction. The non-equilibrium adaptation length L is calculated by Eq.(7).

$$L = \frac{h\sqrt{u^2+v^2}}{\gamma\omega_f} = \max\left[\frac{\mu\theta d_{50}\sqrt{u^2+v^2}}{\alpha\omega_f}, \frac{hC\sqrt{u^2+v^2}}{(1-p)\omega_f}\right] \tag{8}$$

whereμ is a dimensionless coefficient ranging from 6 to; ω_f is the effective setting velocity of sediment particle. In high concentration mixtures, the settling velocity of a single particle is reduced due to the presence of other particles. Considering the hindered settling effect in the fluid-sediment mixture, the formulation of Soulsby (Soulsby 1997) is used.

$$\omega_f = \frac{\nu}{d}\left[\sqrt{10.36^2 + (1-C)^{4.7}1.049d_*^3} - 10.36\right] \tag{9}$$

where d_*=$d_{50}[(s\text{-}1)g/\nu^2]^{1/3}$ is the dimensionless particle parameter.

2.3 Bed Deformation Model

The bed deformation is determined by the volume of sediment entrained and deposited in the flood process. Sediment vertical transfer between active layer and sheet flow layer is closely related to the bed shear stress exerted by the flood water; the erosion occurs when bed shear stress exceeds the critical value, yet sediment stops motion to deposit if sediment rate surpasses its capacity. The morphological evolution equation for non-uniform sediment clasts is written by

$$\frac{\partial z_b}{\partial t} = \frac{1}{(1-p)}\sum_{i=1}^{N}\frac{(q_{bi} - F_i q_{b*i})}{L} \tag{10}$$

2.4 Unstable Bed Avalanching

If the bed slope of a non-cohesive bed becomes larger than the sediment angle of repose, then bed avalanching will occur to form a new bedform with a slope approximately equal to the angle of repose. The updating equation is calculated by

$$\begin{cases} z_{new(i,j)} = z_{i,j} + \sum_{i=1}^{4}\Delta z_i \\ z_{new(i,j+1)} = z_{i,j+1} - \Delta z_1 \\ z_{new(i+1,j)} = z_{i+1,j} - \Delta z_2 \\ z_{new(i+1,j+1)} = z_{i+1,j+1} - \Delta z_3 \\ z_{new(i-1,j+1)} = z_{i-1,j+1} - \Delta z_4 \end{cases} \tag{11}$$

where

$$\Delta z_i = \begin{cases} \frac{\Delta z}{2} \approx sign(\varphi_i)\frac{l_i(\tan|\varphi_i| - \tan\varphi)}{2} & |\varphi_i| > \varphi \\ 0 & |\varphi_i| \le \varphi \end{cases} \quad where\ \ sign(a) = \begin{cases} 1 & a > 0 \\ 0 & a = 0 \\ -1 & a < 0 \end{cases}$$

where l_i = length of two cells in i direction; l_1=dx; l_2=dy; l_3=l_4=$\sqrt{dx^2+dy^2}$.

2.5 Model Solution Procedures

The hydro-morphodynamic model is solved numerically by the advanced Godunov-type finite volume method. For the bed slope source term treatment and wetting/drying, the homogenous flux approach proposed by (Guan et al. 2013b) is applied. Therein, the time scale of bed change is much larger than that of flow movement so that the flow is calculated assuming a "fixed" bed at each time step. An explicit procedure is implemented with restriction of Courant number CFL<1.0. The numerical method is described as: the sediment flux at the interface of two adjacent cells is solved by inserting a middle contact discontinuity wave, S_*; through the assessment of S_*, the sediment flux is determined based on the concentration in the right cell or left cell. Firstly, the first three flux terms are calculated by the HLL scheme expression as follows:

$$\mathbf{E}^*_{LR\,1,2,3} = \begin{cases} \mathbf{E}_L & if\ S_L \geq 0 \\ \mathbf{E}_R & if\ S_R \leq 0 \\ \mathbf{E}^* & otherwise \end{cases} \tag{12}$$

where $\mathbf{E}_L$ =**E**($\mathbf{U}_L$), $\mathbf{E}_R$ =**E**($\mathbf{U}_R$) are the flux and conservative variable vectors at the left and right side of each cell interface. $\mathbf{E}^*$ is the numerical flux in the star region which is calculated by the Eqn.(Toro 2001). To calculate the inter-cell numerical fluxes, a weighted average flux (WAF) total variation diminishing (TVD) method is employed with a flux limiter function. The TVD-WAF scheme is second-order accurate in space and time. Taking the calculation of flux in the x direction as an example:

$$\mathbf{F}^*_{i+1/2,(1,2,3)} = \frac{1}{2}(\mathbf{F}_i + \mathbf{F}_{i+1}) - \frac{1}{2}\sum_{k=1}^{N} sign(c_k)\Phi^k_{i+1/2}\Delta\mathbf{F}^k_{i+1/2} \tag{13}$$

where, $\mathbf{F}_i$= **F** ($\mathbf{U}_i$), $\mathbf{F}_{i+1}$= **F** ($\mathbf{U}_{i+1}$) are the flux and conservative variable vectors at the left and right sides of each cell interface; c_k is the Courant number for wave k, c_k=$\Delta t S_k/\Delta x$; S_k is the speed of wave k and N is the number of waves in the solution of the Riemann problem; $\Phi(r)$ is the WAF limiter function. Based on the solution of the previous three flux terms, the fourth flux term (sediment flux $F_{i+1/2,4}$) is determined by the relationship of the middle waves S_* and zero:

$$F^*_{i+1/2,4} = \begin{cases} F^*_{i+1/2,1}C_L & if\ S_* \geq 0 \\ F^*_{i+1/2,1}C_R & if\ S_* < 0 \end{cases} \tag{14}$$

where C_L and C_R are the volumetric sediment concentration in the left and right cells; $F_{i+1/2,1}$ is the first flux component calculated by Eq.(12). The middle wave speed S_* is calculated by

$$S_* = \frac{S_L h_R(u_R - S_R) - S_R h_L(u_L - S_L)}{h_R(u_R - S_R) - h_L(u_L - S_L)}$$

To update the variables in discretized cells, the finite volume method (FVM) is used.

$$\mathbf{U}^{n+1}_{i,j} = \mathbf{U}^n_{i,j} - \frac{\Delta t}{\Delta x}\left(\mathbf{F}^*_{i+1/2,j} - \mathbf{F}^*_{i-1/2,j}\right) - \frac{\Delta t}{\Delta y}\left(\mathbf{G}^*_{i,j+1/2} - \mathbf{G}^*_{i,j-1/2}\right) + \Delta t\mathbf{S}_{i,j}$$

3 RESULTS AND DISCUSSION

3.1 Dyke Breach Due to Flow Overtopping

The experiment conducted by Université Catholique de Louvain (Spinewine et al. 2004) was reproduced here. The channel flume is 36.2m long and 3.6m wide; and a 2.4m×0.47m sand dyke was built in the location of 11.8m in the flume. The upstream and downstream slopes of sand dyke are 1:2 and 1:3 respectively. A sand layer of 10cm is in the downstream, and the bed material is constituted by sand with median diameter of d_{50}=1.80mm, specific gravity of s=2.615, porosity of p=0.42, as well as angle of repose of φ=34°. The upstream reservoir was separated by a gate before which water is stored. When starting the experiment, the gate is gradually opened so the water filled the second part of the reservoir until water level was 0.45m. A small trapezoidal breach was dug on the top middle of dyke to initiate, the flow overtopping at this point.

3.1.1 Simulated results

For such kind of flood events, outflow peak discharge is a vital hydraulic parameter to be predicted.

The spatial and temporal evolution of the entire flood process can be well simulated in a simple and effective approach, including outflow hydrograph, peak outflow discharge, change of water level, as well as evolution of breach size etc. Manning's n has a direct influence on bed shear stress which decides the quantification of flow-induced sediment, therefore, three Manning's n (n=0.017, 0.018, 0.019) are used respectively for evaluating its sensitivity in the modelling of the dyke breach process. Figure.1 illustrates the comparisons between predicted results and measured data. It can be seen that the Manning's n changes the peak value and the occurrence time of peak outflow discharge, consequently the water level in the reservoir is also changed. According to the comparisons in Figure 1, the presented model predicts the outflow hydrograph and the temporal change of water level in the reservoir with good agreement. Therein, n=0.018 gave a better prediction of the peak discharge.

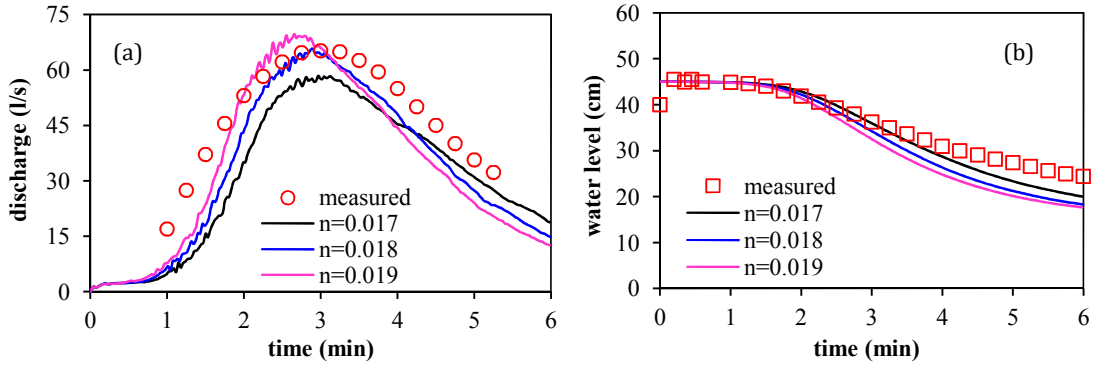

Figure 1 Comparisons of the simulated and measured data: (a) water level in reservoir; (b) outflow discharge

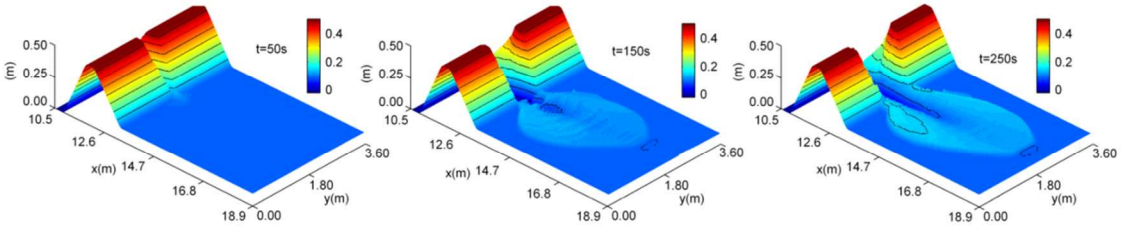

Figure 2 Dyke breach process due to flow overtopping at t=50s, 150s and 250s, respectively

3.1.2 Sediment blockage effects

In order to demonstrate sediment effects on the outflow process, we also run a case with a constant breach on the top of dyke, and the initial breach is assumed as the size at t=6 minutes for the case simulated above. Figure 3(a) shows the comparison of the outflow discharge for 'sudden collapse' of dyke and the case with sediment erosion and deposition. It is clearly indicated that the existence of sediment blocks the flood propagation significantly, not only in terms of the peak discharge, but also the arrival time. For the 'sudden collapse' with a constant breach, the outflow discharge reaches the maximum value immediately when the dyke-breach occurs, and the peak discharge is significantly larger than that with consideration of sediment effects. Thus, we can conclude that sediment play a role of blockage which reduces the peak flow and delays the arrival time. The examples of blockage effects of sediment involve the process of failure of river dyke or landslide dams. In addition, as shown in Figure 3(b), these blockage effects can be found in the numerical and experimental cases of dam-break flow over movable bed (Fraccarollo and Capart 2002). However, based on these insights, we cannot conclude that sediment play a blockage role in the flood events universally, because the insights were obtained by investigating a small-scale special case. The implications of sediment in a large-scale flood will be investigated through modelling a rapid flash flood in reality in the following section.

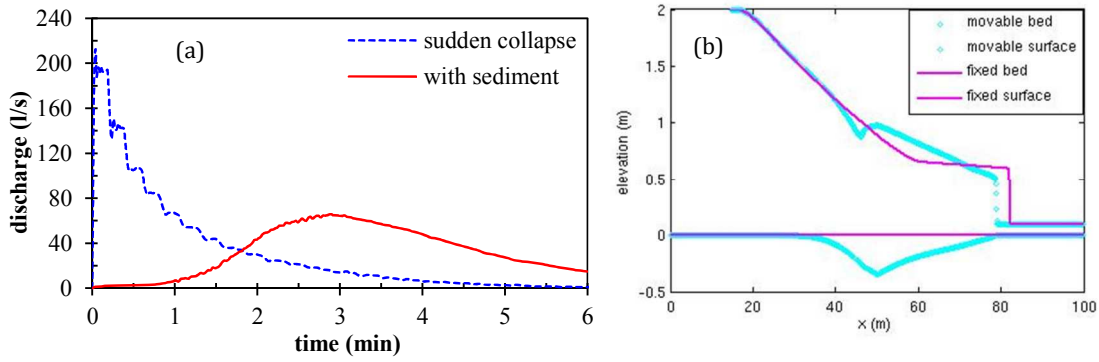

Figure 3 (a) the comparison of outflow discharge for the two different conditions; (b) the comparison of dam-break over movable bed and fixed bed

3.2 Applied to Real-world GLOF Event

3.2.1 Study area

A volcano-induced glacial outburst flood occurred unexpectedly at Sólheimajökull, Iceland in July, 1999 and it was well documented and has been physically investigated in detail (Russell et al. 2010). The river channel is about 9*km* long and 400-700*m* wide. The DEM topography data used here is 8m×8m resolution. The inflow hydrograph is a rapid flood of 6 hours process as shown in Figure 4, and the outflow boundary is free open. The sediment material involves granules (2.8*mm*), cobbles (105*mm*) and boulders (400*mm*) with density of 2680kg/m^3. It is assumed that sediment transport occurs in the mode of sheet flow load which is conventionally referred to as bed-load transport at high bottom shear stress. The model is run in the flood period from 0 hour to 6 hours.

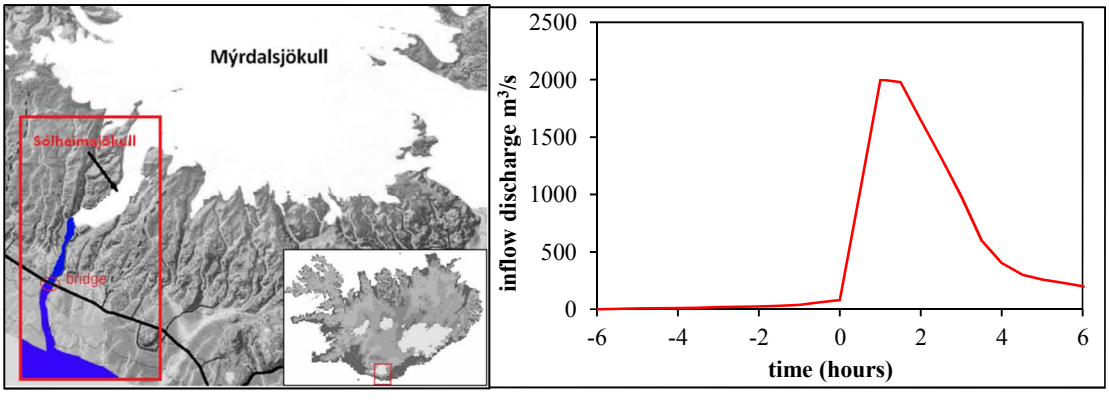

Figure 4 The location of research area (left); the cumulative inflow hydrograph (right)

3.2.2 Hydraulic effects of sediment transport in flood propagation

In this section, the effects of sediment load in the large-scale flood event are discussed. In order to answer this question, two runs are conducted: i) clear floodwater modelling without sediment transport; ii) flood modelling with sediment transport. The temporal change of flow discharge and water elevation at the cross section (x=332908.86) nearby the bridge are selected as a typical one to compare between the two runs as shown in Figure 5. It is indicated that: (1) the maximum water depth with sediment is larger than that without sediment; (2) the arrival time of peak discharge for flooding with sediment is considerably earlier than that without sediment transport, and the is accelerated by approximately 32.7%; moreover, the arrival time of water front is also accelerated due to the incorporation of sediment transport. This insight subverts the understanding mentioned above. Sediment transport accelerates the propagation of water flow in the large-scale flood.

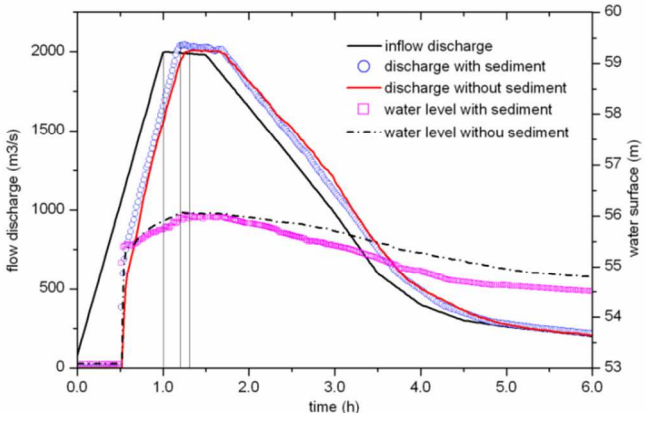

Figure 5 The temporal change of flow discharge and water level at cross section of x=332908.86

Furthermore, in terms of the spatial-scale effects of sediment transport, the differences of maximum water level and water depth at 2 hours of flooding, as well as the final minimum bed elevation between modelling results with and without sediment are illustrated in Figure 6 to further explain the role of sediment in the flooding. It is clearly shown that a primary spatial-effect of sediment is to reduce the maximum water level and water depth at most cross sections, and to increase them at some locations. In addition, Figure 7 illustrates the contour plot of water depths and the differences of water depths and water surfaces with and without sediment in the river channel at 2 hours of flooding. It is indicated that: firstly, the features of water depth are completely different in terms of the quantity and distribution; more specifically, the spatial distribution of water depth with sediment is very smooth and does not have too much oscillation compared to that without sediment, probably because the high intense rapid flow scours the protruding bed and deposits the depressed topography, so that making the irregular topography smoother; secondly, from Figure 7(b), it can be seen that the water surface is reduced at most areas due to sediment transport, as for the water depth, it increases and decreases location-dependently. In summary, we infer that the flood water induces the sediment transport, creating a smoother topography, which conversely leads to the flood propagation to be accelerated. This is also determined as an important reason that the arrival time of peak flow with the incorporation of sediment transport is significantly earlier.

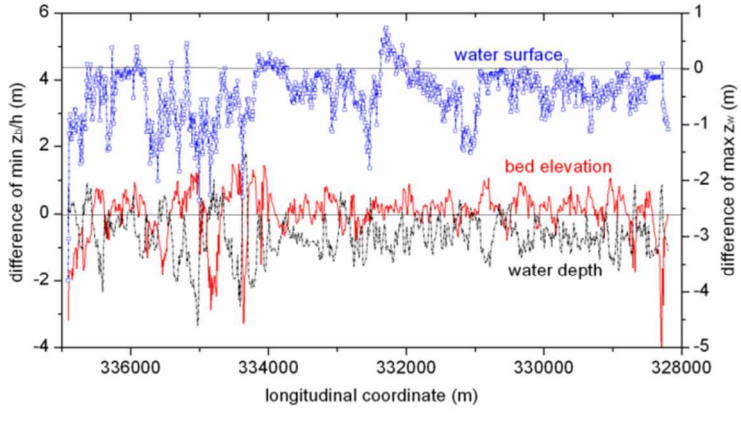

Figure 6 The difference of the maximum water surfaces and the minimum bed elevations between modelling results with and without sediment (note:$\Delta\eta = \eta_{sed} - \eta_{no\ sed}, \Delta h = h_{sed} - h_{no\ sed}, \Delta z = z_{sed} - z_{no\ sed}$)

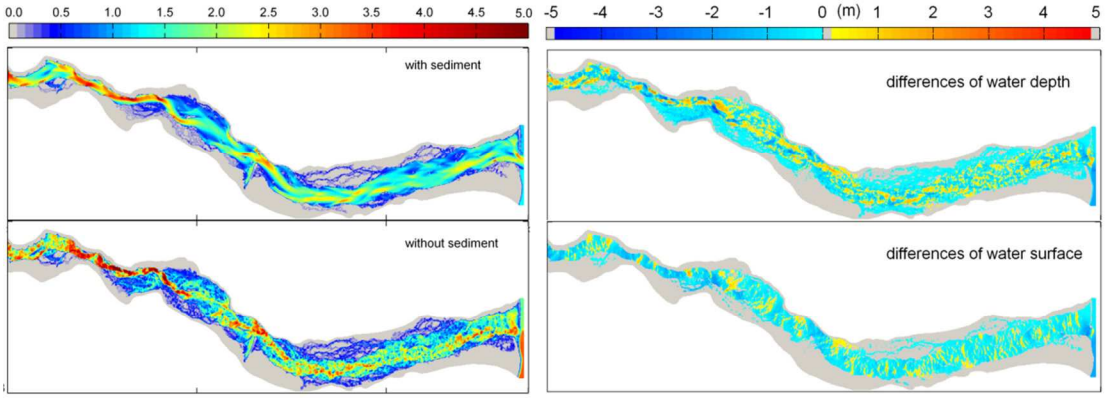

Figure 7(a) the contour plot of water depths with and without sediment; (b) the differences of water depths and water surfaces with and without sediment (note: :$\Delta\eta = \eta_{sed} - \eta_{no\ sed}$, $\Delta h = h_{sed} - h_{no\ sed}$)

3.2.3 Erosion and deposition

The short-lived sudden onset flood induced and carried amount of sediment load, causing the geomorphic change rapidly. The simulated final topography scour is illustrated in Figure 8 showing the spatial distribution of the erosion and deposition at t=20 minutes, 40 minutes, 1 hour, 2 hours, 4 hours and 6 hours since the flood occurs. It is found that the volcano-induced flood causes the erosion and deposition to occur gradually in the main channel, and the erosion and deposition is more severe in the narrower reach of the river, because the narrow channel deepens the water depth and meanwhile elevates the value of velocity, which induces more sediment into movement and correspondingly the sediment load re-deposits within a transport distance. As the inflow discharge is characterized by increasing suddenly to the peak stage and decreasing progressively until 6 hours, the total erosion and deposition volume is closely related to the degree of inflow discharge. It is also noted that the majority of erosion and deposition occur in approximately 2-3 hours that is the period of peak flow discharge, and in conversely, just little scour happens during the flood subsiding time. In summary, we conclude that (1) the rapid outburst flood can induce a rapid geomorphic change; and (2) the erosion rate and deposition rate is closely related to the degree of inflow discharge; (3) the narrower the channel is, the more severe the bed scour.

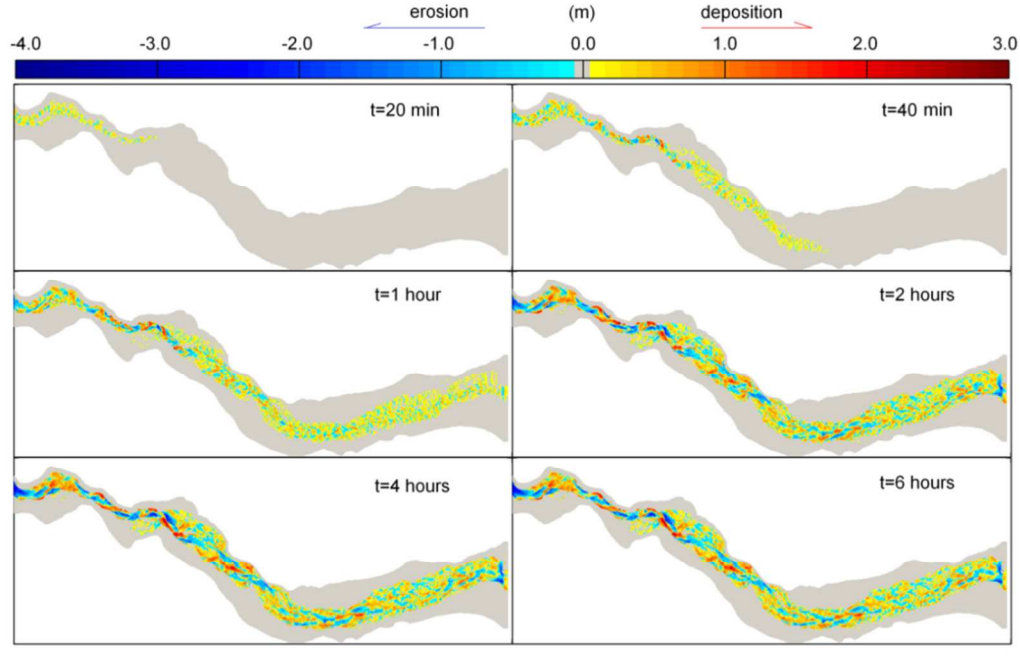

Figure 8 The spatial distribution of geomorphic evolution during the flood process

4 CONCLUSIONS

In general, sediment transport occurs in combination with flood propagation. In this paper, a 2D layer-based sheet flow model was presented and the multiple roles of sediment transport in flash floods were analysed and discussed through simulating a small-scale experiment and a large-scale rapid transient geomorphic flood. Through the analysis of the modelling results, we conclude that on the one hand, sediment can delay the onset of the flood, changing the hydrograph of the flow; on the other hand, for some cases, the flood propagation is significantly accelerated due to the incorporation of sediment transport; conversely, powerful flash floods induce the sediment into motion and cause a rapid morphological change of river bed. Therefore, the rapid flood inundation cannot just focus on the water flow solely. It is necessary to incorporate the sediment transport effects in the inundation modelling. The understanding obtained above is helpful and significant for disaster assessment and flood risk management.

ACKNOWLEDGEMENT

The first author would like to thank the China Scholarship Council (CSC) and the School of Civil Engineering at University of Leeds for their financial support for his PhD studies. We wish to thank Dr. Jonathan Carrivick from School of Geography, University of Leeds for providing the data of the Iceland flood case.

References

Alho P., Russell A.J., Carrivick J.L. and Käyhkö J., 2005. Reconstruction of the largest Holocene jökulhlaup within Jökulsá á Fjöllum, NE Iceland. Quaternary Science Reviews, 24 (22), 2319-2334.

Capart H. and Young D.L., 1998. Formation of a jump by the dam-break wave over a granular bed. Journal of Fluid Mechanics, 372, 165-187.

Carrivick J.L., Manville V., Graettinger A. and Cronin S.J., 2010. Coupled fluid dynamics-sediment transport modelling of a Crater Lake break-out lahar: Mt. Ruapehu, New Zealand. Journal of Hydrology, 388 (3-4), 399-413.

Carrivick J.L. and Rushmer E.L., 2006. Understanding high-magnitude outburst floods. Geology Today, 22 (2), 60-65.

Fraccarollo L. and Capart H., 2002. Riemann wave description of erosional dam-break flows. Journal of Fluid Mechanics, 461, 183-228.

Greimann B., Lai Y. and Huang J.C., 2008. Two-dimensional total sediment load model equations. Journal of Hydraulic Engineering, 134 (8), 1142-1146.

Guan M., Wright N.G., Sleigh P.A., Carrivick J.L. and Staines K., Year. A layer-based morphodynamic model for unsteady outburst geomorphic floods: application in real world events. 10th International Conference on Fluvial Sedimentology, Leeds, UK.

Guan M.F., Wright N.G. and Sleigh P.A., 2013b. A robust 2D shallow water model for solving flow over complex topography using homogenous flux method. International Journal for Numerical Methods in Fluids (10.1002/fld.3795).

Manville V., White J.D.L., Houghton B.F. and Wilson C.J.N., 1999. Paleohydrology and sedimentology of a post-1.8 ka breakout flood from intracaldera Lake Taupo, North Island, New Zealand. Geological Society of America Bulletin, 111 (10), 1435-1447.

Meyer-Peter E. and Müller R., 1948. Formulas for bed load transport. . Proc, 2nd Meeting, IAHR, Stockholm, Sweden,, 39–64.

Russell A.J., Tweed F.S., Roberts M.J., Harris T.D., Gudmundsson M.T., Knudsen Ó. and Marren P.M., 2010. An unusual jökulhlaup resulting from subglacial volcanism, Sólheimajökull, Iceland. Quaternary Science Reviews, 29 (11–12), 1363-1381.

Smart G. and Jäggi M., 1983. Sediment transport on steep slopes. Mitteilung 64 Versuchsanstalt fu¨ r Wasserbau, Hydrologie und Glaziologie, ETH Zurich, Zurich.

Soulsby R., 1997. Dynamics of marine sands: a manual for practical applications. ThomasTelford, London, UK.

Spinewine B., Delobbe A., Elslander L. and Zech Y., Year. Experimental investigation of the breach growth process in sand dikes. Proceedings of the Second International Conference on Fluvial Hydraulics, Napoli, Italy.

Toro E.F., 2001. Shock-Capturing Methods for Free-Surface Shallow Flows John Wiley &Sons, LTD.

Wu W.M. and Wang S.S.Y., 2007. One-dimensional Modeling of dam-break flow over movable beds. Journal of Hydraulic Engineering, 133 (1), 48-58.

Xia J., Lin B., Falconer R.A. and Wang G., 2010. Modelling dam-break flows over mobile beds using a 2D coupled approach. Advances in Water Resources, 33 (2), 171-183.